Rapid Expansion of Cellulose Triacetate from Ethyl Acetate Solutions

A. Blasig, M. C. Thies

Center for Advanced Engineering Fibers and Films, Department of Chemical Engineering, Clemson University, Clemson, South Carolina 29634-0909

Received 15 August 2003; accepted 28 May 2004
DOI 10.1002/app.21201
Published online in Wiley InterScience (www.interscience.wiley.com).

ABSTRACT: Rapid-expansion-of-supercritical-solution (RESS) experiments were performed for solutions of cellulose triacetate [CTA; weight-average molecular weight = 145,700, polydisperity = 2.07] in ethyl acetate [EA] over a range of concentrations and conditions of polymer–solvent phase behavior. Solid-solubility experiments were carried out beforehand and identified hot and compressed liquid EA at approximately 175°C as a good solvent for CTA. Cloud-point measurements were then used to locate the region of liquid–liquid equilibrium (LLE) for this system. The RESS results indicate that the phase state of the pre-expansion mixture determines the product size, and the overall concentration of the pre-expansion mixture determines the product morphology. However, we have also discovered a new constraint: for the production of well-formed fibers and particles, the rapid-expansion path must include penetration into a region of LLE, which must exist over a sufficient pressure range so that a separate, polymer-rich liquid phase has time to develop before the onset of vapor–liquid equilibrium (VLE). If rapid expansions are carried out at temperatures near or below the lower critical end point, the expansion path leads directly into a region of VLE, and a disruptive vapor expansion occurs within the continuous liquid phase. In this case, hollow particles, hollow structures, and even foams are produced. By the proper choice of operating conditions, we were able to produce continuous CTA fiber from a 5 wt % solution in EA at 250°C and 69 bar. © 2004 Wiley Periodicals, Inc. J Appl Polym Sci 95: 290–299, 2005

Key words: fibers; phase behavior

INTRODUCTION

When a supercritical fluid containing a dissolved polymer is rapidly expanded across a nozzle to ambient pressures, the solvent density decreases dramatically, and the solute precipitates from solution. Because the process occurs under transonic conditions, residence times in the nozzle are approximately 10^{-6} s, leading to high supersaturation ratios in the postexpansion environment. Petersen et al.[1] were the first to call this process the rapid expansion of supercritical solutions (RESS). RESS has been used to process polymers into a wide variety of morphologies, including submicrometer- and micrometer-sized particles,[1–7] films,[8,9] and even fibers.[2,10–14]

Several research groups have investigated the effect of RESS processing conditions, such as the nozzle geometry and pre-expansion temperature (T_{pre}) and pressure (P_{pre}), on the product size and morphology of polymers. In their work with several supercritical-fluid/polymer systems, Lele and Shine[11] and Mawson et al.[12] both concluded that particles are formed from unsaturated solutions and fibers are formed from saturated, two-phase mixtures. No significant impact of the polymer concentration on the product morphology was reported; however, the investigated solutions were relatively dilute, never exceeding 2 wt % polymer. Aniedobe and Thies[13] were the first to report a relationship between the polymer concentration and product morphology, as they observed a transition from continuous fibers to particles as the cellulose acetate concentration in supercritical methanol decreased from approximately 10 wt % to less than 1 wt % over the course of their experiments. Blasig et al.[14] systematically investigated the effects of the concentration and phase state on the RESS of solutions of CO_2 and poly(heptadecafluorodecyl acrylate), a CO_2-soluble fluoropolymer. The results were consistent with those of Aniedobe and Thies,[13] in that fibers were produced from higher concentrations (i.e., 5 wt %) and particles were produced from lower concentrations (i.e., 0.5 wt %) independently of the phase state of the polymer–solvent mixture. Instead, the phase state was found to affect the product size, with smaller structures formed from homogeneous solutions and larger ones formed from two-phase mixtures.

Correspondence to: M. C. Thies (mcths@clemson.edu).
Contract grant sponsor: National Science Foundation (through the ERC program); contract grant number: EEC-9731680.

In this work, we report on the rapid expansion of cellulose triacetate (CTA) from near-critical and supercritical solutions of ethyl acetate (EA; critical temperature = 250.0°C; critical pressure = 38.3 bar). Although CTA is insoluble in EA at ambient temperatures, previous work has shown that the use of hot or supercritical conditions can dramatically improve polymer solubility in a given solvent.[13] Major uses for CTA include textile fibers and as the base for photographic film.[15] In addition, hollow-fiber membranes of CTA are used for both hemodialysis and desalination applications.[16] The most common solvent system for processing CTA fibers and films contains up to 95% methylene chloride,[17] and therein lies the problem. Because methylene chloride is a probable carcinogen with its own comprehensive Occupational Safety and Health Administration health standard, CTA production in the United States has been severely curtailed over the past decade, with most production being moved offshore.[17,18] Clearly, there is a need for nontoxic solvents for CTA processing.

The objectives of this study were to (1) identify a nontoxic solvent for CTA processing, (2) determine the product morphologies produced by RESS processing of CTA with the nontoxic solvent, and (3) determine the general applicability of the relationships between the RESS processing conditions and product characteristics that were established in our previous work.

EXPERIMENTAL

Materials

EA was supplied by Fisher Scientific (Pittsburgh, PA; high-performance-liquid-chromatography-grade, 99.9% purity) and was stored in a clean and dry 1-L bottle together with approximately 100 g of a 3-Å molecular sieve (Mallinckrodt, Hazelwood, MO; grade 564, 3-Å, 8–12-mesh) for the removal of any residual water. The molecular sieve had been previously regenerated by being held for 24 h at 200°C under a continuous purge of dry nitrogen. Each time a solvent bottle was opened, the overhead space was purged with dry nitrogen for 1–2 min before the bottle was closed. A gas chromatograph (HP 6890, Hewlett–Packard, Palo Alto, CA) equipped with a mass spectrometer (model 5973, Hewlett–Packard) and a 100% poly(ethylene glycol) column (part no. 19655, Alltech, Deerfield, IL; 30 m long with a 0.25-mm i.d. and a 0.25-μm film thickness) was used to periodically determine the EA purity, which typically was 99.90% (including water). Nitrogen was obtained from National Welders (Charlotte, NC; industrial-grade, 99.995% pure).

CTA (see Fig. 1) was purchased from Aldrich (Milwaukee, WI). The polymer was determined to be semicrystalline by X-ray powder diffraction (model XDS-2000, Scintag, Inc., Cupertino, CA), to have a melting temperature of 295°C by differential scanning calorimetry (model DSC 820, Mettler–Toledo, Inc., Columbus, OH), and to be stable up to approximately 305°C by thermogravimetric analysis (model TGA/SDTA 851, Mettler–Toledo). The weight-average molecular weight (M_w = 145,700 g/mol) and polydispersity [weight-average molecular weight/number-average molecular weight (M_w/M_n) = 2.07] of CTA were determined for us by American Polymer Standards Corp. (Mentor, OH) with gel permeation chromatography. The mobile phase, methylene chloride, was pumped at a flow rate of 1 mL/min at 30°C through two in-series, mixed-bed columns (AM Gel Linear/10, American Polymer Standards, Mentor, OH) followed by a refractive-index detector. The reported molecular weights were based on a reference calibration curve obtained from a single broad CTA standard with M_w = 140,000 g/mol and M_w/M_n = 2.47 (CTA140K, American Polymer Standards).

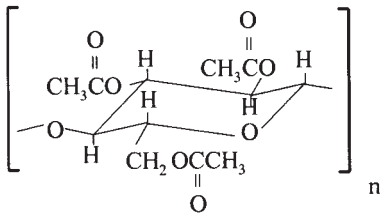

Figure 1 Molecular structure of CTA.

Phase-behavior measurements

A variable-volume view cell was used for two types of phase-behavior measurements: (1) determining whether solid CTA would dissolve in the solvents of interest and (2) measuring polymer–solvent liquid–liquid equilibrium (LLE) phase boundaries (commonly called cloud-point curves). Cloud-point curves establish the limits of saturation, and as discussed earlier,[2,14] the phase state of the polymer–solvent mixture is a key processing variable in the rapid-expansion process. A schematic of the phase-behavior apparatus used to carry out the aforementioned measurements is shown in Figure 2. This apparatus has been described in detail elsewhere,[14] so only a brief description is given here. The central feature of the apparatus is a variable-volume view cell[19] (316 stainless steel, 26.67 cm long with a 1.59-cm i.d.), which is nominally rated to 1380 bar at 150°C. Because cloud-point measurements were performed up to 235°C, Teflon O-rings and backup rings were used, and the operating pressures never exceeded 350 bar. A pressure generator (model 81-5.75-10 high-pressure equipment, Co., Erie, PA) that is connected to the end of the view cell

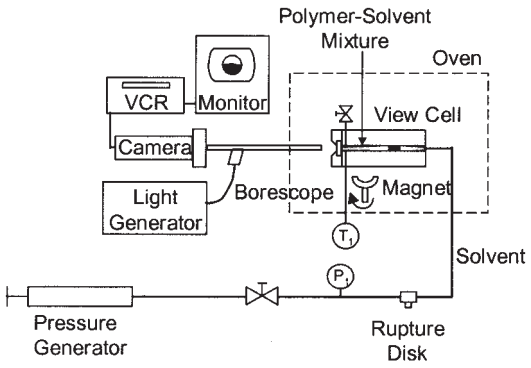

Figure 2 Apparatus for measuring the polymer–solvent phase behavior.

uses the solvent as a working fluid and moves the piston to compress the polymer solution on the other side of the piston. A nitrogen-purged convection oven, designed and constructed at Clemson, provides a constant-temperature environment for the view cell. A borescope with a light generator (Olympus Industrial, Orangeburg, NY) is positioned in front of the view port for observing the polymer solution inside the cell. A charge-coupled device camera (model XC-999, Olympus) attached to the borescope displays the contents of the cell on a monitor, and a videocassette recorder (VCR) is used for recording.

For solubility measurements, the view cell was charged with 0.5–0.7 g of CTA to an accuracy of ±0.0005 g as determined gravimetrically. The solvent (12–14 g) was then charged to the cell to an accuracy of ±0.01 g; the higher uncertainty was due to the evaporation of the solvent during weighing and charging. After the space (which was kept below ~10 μL) was purged above the polymer–solvent mixture with low-pressure nitrogen, the view cell was sealed. The cell was then placed inside the oven, and pressurized to 345 bar with the pressure generator. After 20 min of continuous mixing, the solid polymer inside the cell was observed to remain undissolved at room temperature. The oven was then used to heat the view cell at a rate of approximately 2°C/min, while the pressure was controlled at 345 bar with the pressure generator. An atmosphere of less than 2% oxygen was maintained inside the oven by low-pressure nitrogen purging to prevent an explosion hazard should a cell leak occur. The polymer–solvent mixture inside the view cell was continuously mixed and monitored until a homogeneous solution was obtained at elevated temperatures.

For cloud-point measurements, the view cell was charged as described previously and to the same accuracy, but with 0.08–1.00 g of CTA and 8.5–25.5 g of the solvent. As for the solubility measurements, the cell was initially heated at approximately 2°C/min at a pressure of 345 bar until a homogeneous, transparent solution was obtained. The temperature increase was then slowed to 0.1–0.5°C/min. (We did not measure cloud points under isothermal conditions because at the elevated temperatures of interest, the Teflon O-rings had a limited lifetime before they would begin to leak.) To determine cloud-point pressures, the pressure was incrementally decreased during continuous mixing until a cloudy solution was obtained. If no clouding of the solution was found above the vapor pressure of the solvent, no cloud point existed at this temperature. In this work, the cloud-point pressure was defined as the pressure at which the piston inside the view cell first became invisible because of the cloudiness of the mixture when the pressure was lowered.

The pressure inside the view cell was determined indirectly by the measurement of the pressure of the working fluid; the pressure drop across the piston was less than 0.7 bar. A calibrated 0–5000 psig pressure gauge, accurate to ±0.25 bar, was used (P_1; model CM-130047, Heise, Newtown, CT). The temperature in the view cell (T_1) was measured with a platinum resistance thermometer (model WSPOG1-4½-5C, Burns Engineering, Minnetonka, MN) to an accuracy of ±0.25°C. With cloud points being measured under nonisothermal conditions, we estimated the accuracy of our reported results to be ±1.5 bar and ±1.5°C. Finally, as a safety measure, a rupture disk was placed downstream of the pressure generator to prevent accidental overpressuring of the system.

Rapid-expansion experiments

A schematic of the rapid-expansion apparatus is shown in Figure 3. The phase-behavior and expansion apparatuses shared the same view cell, convection oven, and borescope setup. A syringe pump (model 500D, Isco, Lincoln, NE) was connected to both ends of the view cell, as the fluid inside the pump served as

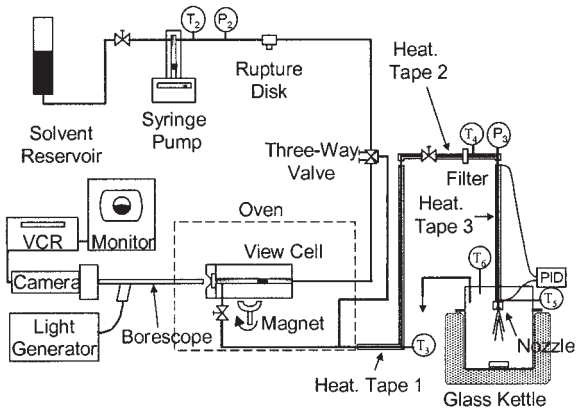

Figure 3 Apparatus for performing rapid-expansion experiments.

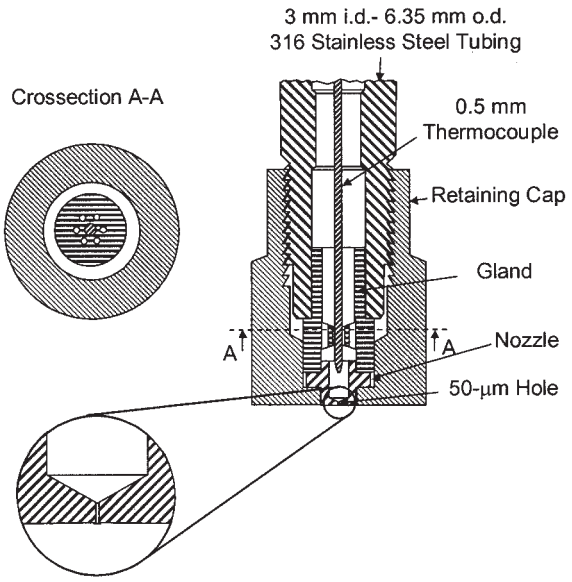

Figure 4 Geometry of the type-II nozzle used in rapid-expansion experiments.

the solvent and as the working fluid. Two different nozzle designs (type I and type II) were used. The type-I nozzle was used in our previous work[14] and had a pinhole 50 μm in diameter and an aspect ratio of approximately 5. A 1.59-mm-o.d. type-K thermocouple (T_5 in Fig. 3) was located inside the pre-expansion tubing about 2 mm upstream of the nozzle to measure T_{pre}. The type-II nozzle had a more complex geometry (see Fig. 4). Its pinhole (50 μm in diameter and an aspect ratio of ~5) was manufactured by electrical discharge machining (Optimation, Inc., Midvale, UT), which produced a cleaner and more accurate bore, and was preceded by a cone-shaped inlet. The retaining cap finished level with the pinhole when tightened onto the pre-expansion tubing (15.24 cm long with a 0.3-cm i.d. and a 0.635-cm o.d.). This design minimized the accumulation of expanded polymer around the nozzle outlet. T_{pre} was measured with an ultrathin, 0.5-mm-o.d. type-K thermocouple (Thermocoax, Alpharetta, GA; T_5 in Fig. 3) located inside the pre-expansion tubing about 2 mm upstream of the nozzle. The thermocouple was centered inside the tubing with a gland. Two heating tapes were wrapped around the tubing between the oven and the pre-expansion section. Power to the heating tapes was supplied by time-proportional power controllers (model PL312 Minitrol, Glas-Col, Terre Haute, IN). Type-K thermocouples were inserted into the tubing at two locations (T_3 and T_4 in Fig. 3) to monitor the temperature. A third heating tape was wrapped around the pre-expansion section and was connected to a proportional-integral-derivative controller (model CN 76000, Omega Engineering, Stamford, CT) that used thermocouple T_5 as the input. With this arrangement, T_{pre} was controlled to within ±3.5°C.

P_{pre} was controlled by the syringe pump to within ±0.35 bar and was measured with a calibrated 0–10,000 psig pressure gauge (labeled P_2; model CM-109834, Heise) located upstream of the nozzle; the pressure measurements were accurate to ±1.0 bar. A 0.5-μm filter (part no. 9200, Alltech) was used to prevent clogging of the nozzle due to impurities. A second pressure gauge (P_3; McDaniel Controls, Inc., Luling, LA) was used to verify that the pressure had not changed significantly because of possible plugging of the filter.

For a typical rapid-expansion experiment, the view cell was charged with 0.1–1.5 g of CTA and 20–36 g of the solvent in the same manner and with the same accuracy as for the phase-behavior measurements. After the cell was secured inside the convection oven, the contents of the cell were compressed with the solvent (now used as the working fluid) from the syringe pump to the desired pressure. The convection oven was heated to approximately 185°C during magnetic stirring of the mixture at the desired P_{pre} value. Once a homogeneous solution was obtained, the pure solvent was delivered from the pump and expanded through the nozzle; the view cell was bypassed by means of the three-way valve (see Fig. 3), and a constant pressure was maintained on the working-fluid side of the view cell. The expansion was into a 500-mL glass kettle that had been preheated with a heating mantle (Glas-Col), and that was maintained at ambient pressure and a temperature of approximately 100°C to prevent condensation of the solvent. The pure-fluid expansion continued until steady state was achieved both at the nozzle and within the kettle; this usually took about 25 min.

To initiate actual rapid-expansion experiments, we diverted the pure solvent flow exclusively to the working-fluid side of the view cell by means of the three-way valve; then we opened the valve on the process side of the view cell, pushing the polymer–solvent solution out of the cell and through the nozzle. The gasified solvent was withdrawn out the top of the kettle, and the polymer precipitate was collected onto an aluminum scanning electron microscopy (SEM) specimen stage covered with carbon tape that had been placed in the bottom of the kettle. A sample was collected onto the stage for about 1 min about 10 cm downstream of the nozzle. The aforementioned procedure was repeated with another glass kettle/specimen stage setup (including kettle preheating to prevent any solvent condensation), and a second sample was collected. The samples were then platinum-coated (model Hummer 6.2, Anatech, Ltd., Battle Creek, MI), and the size and morphology of the precipitate were determined with SEM (model SEM S3500N, Hitachi, Pleasanton, CA). After the experiment, the lines of the expansion apparatus were flushed with the solvent for more than 45 min to remove any residual polymer.

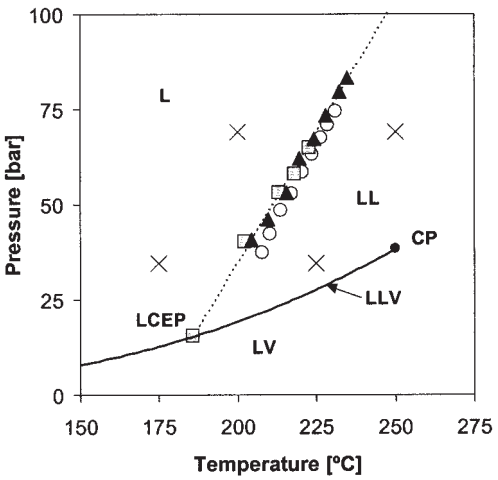

Figure 5 Cloud-point curves for CTA in EA at (○) 0.5, (■) 2, and (▲) 5 wt %. Also shown are (×) the rapid-expansion experiments for CTA in EA at 0.5, 2. and 5 wt %. The vapor pressures for pure EA (—) are from ref. 20.

RESULTS AND DISCUSSION

Phase behavior and chemical stability

Initial solubility measurements were carried out with hot liquid ethanol as a solvent for CTA. Although ethanol completely dissolved CTA at approximately 165°C, a gas chromatography/mass spectrometer (GC–MS) analysis of the solvent recovered after the experiment revealed the presence of approximately 10 wt % EA, which was most likely produced by nucleophilic substitution of the acetate group on CTA with an alcohol. With reactions occurring to such a significant extent, no additional work with ethanol as a solvent for CTA was performed.

Next, EA was evaluated as a solvent for CTA because of its nontoxicity [the U.S. Food and Drug Administration considers EA to be a GRAS (generally regarded as safe) substance], its chemical similarity to CTA, and because any nucleophilic substitution that took place would cause no change in the chemical makeup of CTA or the solvent. For the solubility measurements, liquid EA maintained above its vapor pressure was found to completely dissolve CTA at approximately 175°C. During the heating of the polymer–solvent mixture from ambient temperatures, initial polymer swelling occurred at approximately 145°C. The plasticized polymer beads then fell apart into smaller structures at approximately 170°C and dissolved steadily until they disappeared, leaving a clear solution at approximately 175°C. LLE (i.e., cloud-point) pressures for CTA in EA are shown in Figure 5 from 185 to 235°C for polymer concentrations of 0.5, 2, and 5 wt %. The cloud-point curves show typical lower critical solution temperature (LCST) behavior with a constant cloud-point slope, $(\delta P/\delta T)_x$, of approximately 1.4 bar/°C for all temperatures and polymer compositions investigated. From our cloud-point measurements, we have estimated that the lower critical end point (LCEP)[21] for this system occurs at 186 ± 2°C and 15.5 ± 2 bar. An analysis of the recovered solvent by GC–MS showed no changes in the EA purity from the initial charge. Furthermore, Fourier transform infrared analysis indicated that the recovered polymer still consisted exclusively of CTA.

Our recent collaboration with Enick and coworkers at Pittsburgh[22] has elucidated the global phase behavior exhibited by solvents with melting points above the critical points of the solvents. On the basis of this work and our cloud-point measurements, we propose the pressure–concentration–temperature diagram shown as Figure 6 for the CTA–EA system. For simplicity, we assume in the diagram that CTA is monodisperse. Above the LCEP at 186°C, the LLE region dominates the pressure–concentration phase diagram, although the solid–liquid (SL) region probably extends to relatively high concentrations of EA at temperatures near the LCEP.[22] At temperatures below the LCEP, the only observed fluid-phase behavior is vapor–liquid equilibrium (VLE), with a three-phase SLV line and a region of SV equilibria both existing at lower pressures. Projections of the maximum-pressure points of LLE (i.e., the cloud-point pressures) onto the pressure–temperature plane on the left side of the diagram form the critical locus curve known as the LCST curve, which is shown in Figure 6 as a dashed line. Thus, the phase behavior is type V according to the classification system of Scott and van Konynenburg.[23] This classification system does not consider the SLV and SV behavior that exists at lower pressures[22] and was not measured in this work.

Finally, an interesting kinetic phenomenon was observed upon the cooling of homogeneous mixtures of CTA and EA that had been formed at elevated temperatures and pressures: once dissolved in EA, CTA remained in solution upon its return to ambient conditions. However, once the solvent was removed from

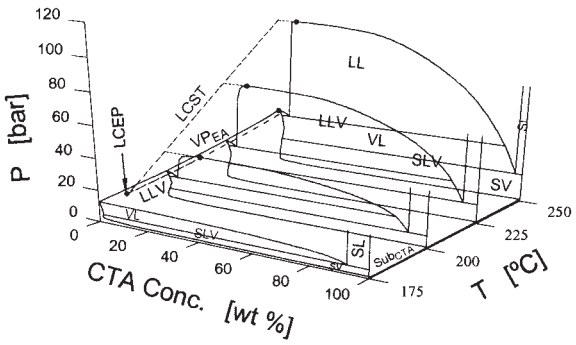

Figure 6 Proposed pressure–temperature–composition diagram for the CTA–EA system at 175, 200, 225, and 250°C. The vapor pressures for pure EA (VP_{EA}) are from ref. 20. All other lines are qualitatively represented.

CTA, the polymer again became insoluble in ambient-temperature EA. CTA solutions that were recovered after phase-behavior measurements formed gels within several days for 5 wt % CTA and within weeks for 0.5 and 2 wt % solutions.

Rapid-expansion experiments

As shown in Figure 5, T_{pre} and P_{pre} were selected on the basis of the measured cloud-point curves, such that both unsaturated, homogeneous liquids and saturated, two-phase liquid–liquid mixtures were expanded. An upper temperature limit of 250°C was chosen because of the limitations of the O-rings in our view cell and to stay safely below the polymer degradation temperature (i.e., ~305°C). For each of the four pre-expansion conditions shown, polymer concentrations of 0.5, 2, and 5 wt % were investigated to give a total of 12 experimental runs; 3 of these runs were duplicated to check reproducibility.

We were concerned that reduced flow rates due to partial plugging of the orifice with the polymer could affect the product morphology. Thus, the flow rates were first measured with pure EA to determine the rates for an unobstructed orifice. The flow rates were monitored during actual expansion experiments with CTA, and those few experiments that exhibited reduced flow rates due to partially obstructed orifices were terminated and rerun.

Mixtures of CTA and EA were first expanded with the type-I nozzle. Unfortunately, this nozzle design allowed CTA to precipitate onto the retaining cap and then grow into the free-jet region. This penetration of precipitate into the free jet was not observed in our previous work.[14] Although expansion through a type-II nozzle (Fig. 4) still led to the precipitation of CTA onto the retaining cap, the rate of accumulation was much slower, and so the precipitate did not grow enough to penetrate the expansion jet. Thus, all the reported experiments were carried out with the type-II nozzle.

Typical rapid-expansion morphologies from hot and near-critical solutions collected about 10 cm downstream of the type-II nozzle are presented in Figures 7–9. As shown in Figure 7(a), the expansion of a homogeneous, unsaturated solution containing 0.5 wt % polymer yielded small, 0.1–0.5-μm spheres, hollow particles of 0.5–5.0 μm, and irregularly shaped structures of 1–15 μm; the last appeared to consist of numerous small particles fused together. On the other hand, the expansion of a two-phase, 0.5 wt % mixture produced larger, 0.5–1.5-μm spheres [Fig. 7(b)]. Unlike the expansion of the homogeneous solution, only small amounts of other structures were produced. Similar behavior was observed at a 2 wt % concentration [see Fig. 8(a,b)], as both spheres (0.1–0.5 μm) and hollow structures (0.5–20.0 μm) were produced from

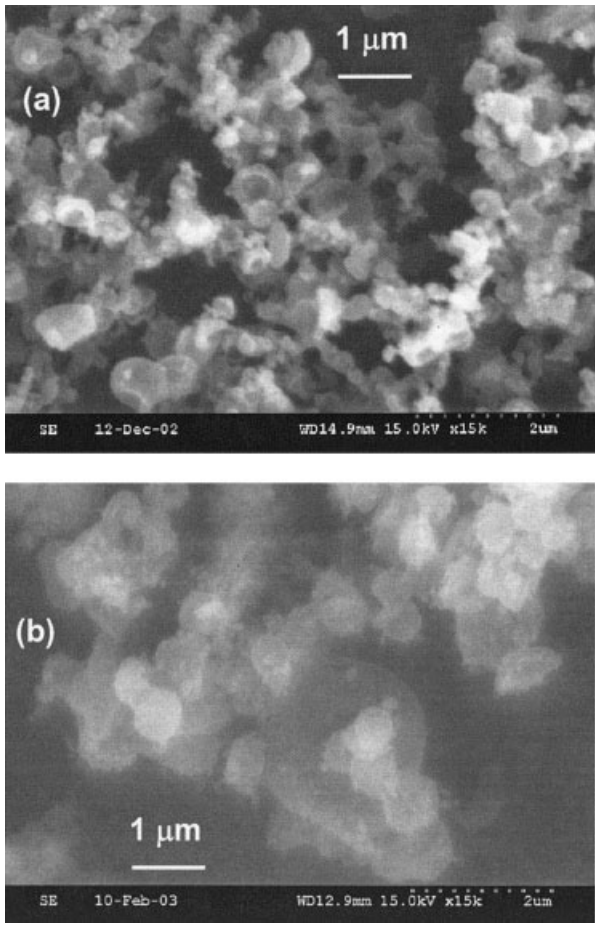

Figure 7 SEM micrographs of rapid-expansion products obtained from a 0.5 wt % CTA solution: (a) T_{pre} = 200°C, P_{pre} = 69 bar, and an unsaturated solution, and (b) T_{pre} = 250°C, P_{pre} = 69 bar, and a two-phase mixture.

the homogeneous solution, but 0.5–1.5-μm spheres were the dominant structure from the expansion of the two-phase mixture. As shown in Figure 9, increasing the concentration to 5 wt % resulted in the formation of fibers, regardless of the phase state of the mixture being expanded. For homogeneous solutions, 0.1–0.5-μm submicrometer fibers were produced [Fig. 9(a)]; for two-phase mixtures, larger, 0.5–20.0-μm fibers were formed [Fig. 9(b)]. Many larger, hollow structures (0.5–20.0 μm) were also obtained upon the expansion of the homogeneous solution [Fig. 9(a)]. Figure 10 shows the product collected from a 5 wt % CTA–EA solution under pre-expansion conditions of 250°C and 69 bar on a macroscopic scale; the morphology is reminiscent of a cotton ball. Clearly, the rapid expansion of EA solutions can be used to produce large amounts of continuous CTA fibers.

All samples investigated in this work also contained small amounts of fibers, 0.1-μm spheres, and large particles ranging from 50 to 250 μm. The larger particles were the result of the accumulation of CTA on the retaining cap of the expansion nozzle, followed by

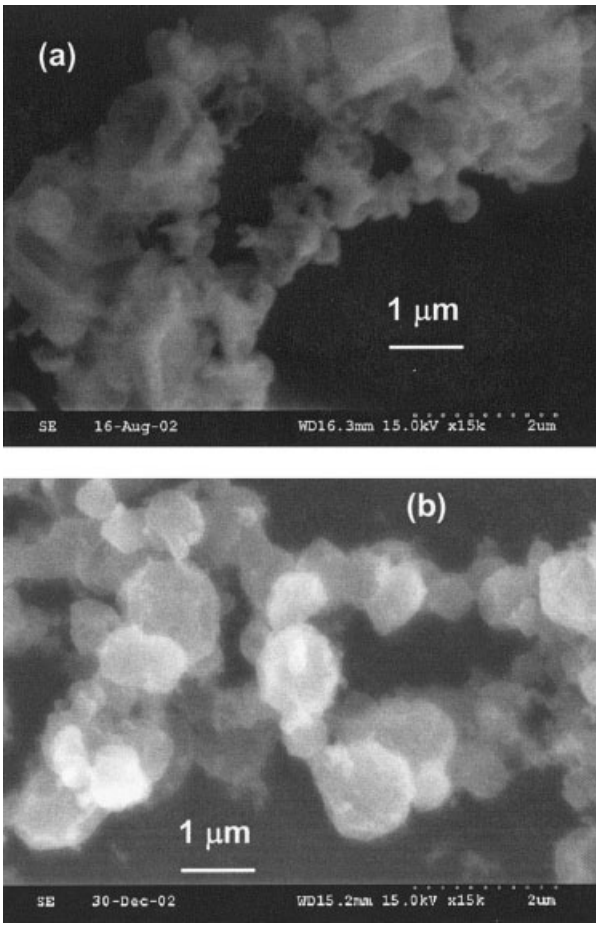

Figure 8 SEM micrographs of rapid-expansion products obtained from a 2 wt % CTA solution: (a) T_{pre} = 200°C, P_{pre} = 69 bar, and an unsaturated solution, and (b) T_{pre} = 250°C, P_{pre} = 69 bar, and a two-phase mixture.

their dropping into the sample. For all three of the experiments that were duplicated in this work, reproducible results were obtained. Detailed information on all experimental runs is presented elsewhere.[24]

In summary, the behavior of CTA–EA solutions processed by rapid expansion is similar to what was previously observed in our work with poly(HDFDA) with CO_2:[14] (1) the phase state of the mixture under pre-expansion conditions determines the product size, with smaller morphologies being produced from homogeneous solutions rather than two-phase mixtures, and (2) the overall polymer concentration in the pre-expansion mixture determines the product morphology, with particles dominating at lower concentrations (0.5 and 2 wt %) and fibers dominating at higher ones (i.e., 5 wt %). An exception to these general trends occurred under pre-expansion conditions of 175°C and 35.5 bar: large (~1 cm) structures were created by a foaming-dominated product morphology. This exception is addressed later.

To qualitatively explain the results of our rapid-expansion experiments, we have plotted the process path on a pressure–concentration (P–x) phase diagram, as shown in Figure 11 (this figure was obtained from isothermal cuts of Fig. 6). Although it is overly simplistic to assume that the rapid-expansion process occurs under isothermal conditions (as a significant degree of cooling will occur for any rapid expansion that uses a short orifice[25]), this assumption will still allow us to identify the various phase transitions that can occur during rapid expansion.

Figure 11(a) is a P–x diagram for the CTA–EA system at 200°C; plotted on the figure is an isothermal rapid-expansion path for a typical polymer concentration (e.g., 2 wt %). The illustration to the right depicts the phase transitions that occur along the expansion path, with the numbers next to the illustration corresponding to the numbered points on the P–x diagram. Generally, a new phase is formed when a pressure drop results in a phase boundary being crossed. Initially, nuclei of the new phase are formed within the original phase; these nuclei then grow either by condensation (the precipitation of matter from the original phase onto the nuclei) or by coagulation (the merging of two new phase volumes).

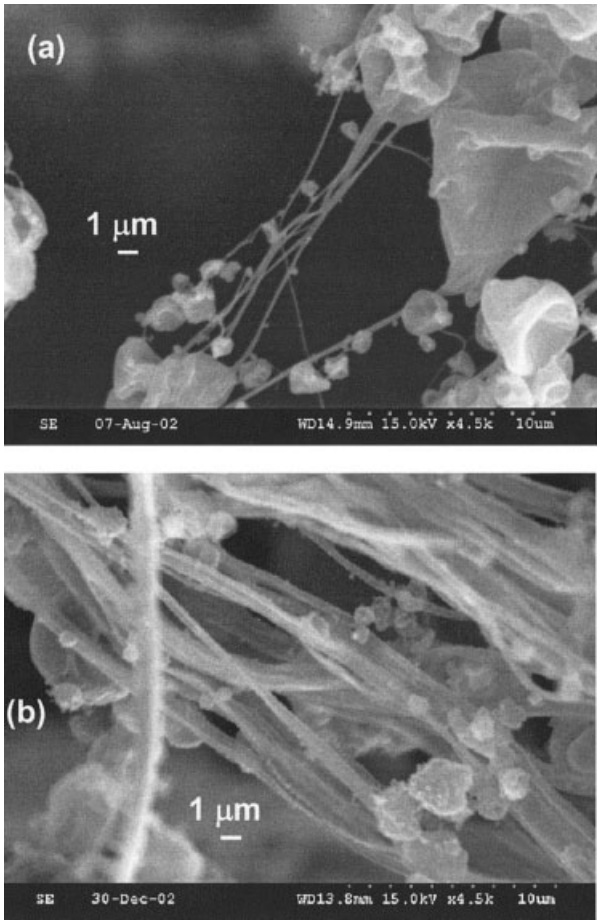

Figure 9 SEM micrographs of rapid-expansion products obtained from a 5 wt % CTA solution: (a) T_{pre} = 200°C, P_{pre} = 69 bar, and an unsaturated solution, and (b) T_{pre} = 225°C, P_{pre} = 34.5 bar, and a two-phase mixture.

Figure 10 Continuous CTA fibers produced by the rapid expansion of a 5 wt % solution in EA under pre-expansion conditions of 250°C and 69 bar.

Starting with a homogeneous solution [i.e., at point 1 in Fig. 11(a)], rapid expansion follows a constant-composition path to lower pressures, at which a polymer-rich liquid phase (L_2) forms within the original solvent-rich liquid phase (L_1) when point 2 is reached. At lower pressures, for example, at point 3, the amount of the L_2 phase is significant. At the three-phase line (point 4), a solvent-rich vapor phase (V) forms from the solvent-rich liquid phase L_1. The L_1 phase boils away at the three-phase pressure until it is completely consumed. With only vapor and polymer-rich liquid (L_2) remaining, the pressure then drops below point 4 [e.g., 5 in Fig. 11(a)]. A solid polymer phase (S) then forms from the polymer-rich liquid phase at point 6 on the three-phase SL_2V line. Because CTA is semicrystalline, the solid phase is created not only by nucleation and growth (to form crystals) but also by vitrification (to form an amorphous phase). Finally, with only vapor and solid remaining, the rapid-expansion path ends at the ambient pressure (i.e., at point 7).

The *P–x* phase diagrams at 225 and 250°C are conceptually identical to the one described previously for 200°C (see Fig. 6). The higher the temperature is, the larger the L_1L_2 region is, so the L_2 phase has more time to develop during the expansion process before vapor-phase formation occurs at the L_1L_2V line (see Figs. 5 and 6). However, for T_{pre} = 175°C, a vapor phase instead of a polymer-rich liquid phase is first created within the original homogeneous phase (i.e., L_1), as we are below the LCEP temperature [see Figs. 5 and 11(b)].

Consider now the rapid expansion of an unsaturated, homogeneous solution. The nucleation of a polymer-rich liquid phase will not occur until a significant pressure drop has occurred inside the nozzle. With the mixture passing through the nozzle in approximately 10^{-6} s, little time exists for the critical nuclei to grow by condensation and coagulation before the formed structures solidify when the pressure drops below the SL_2V line. With so little time available for growth, small structures are formed.

The hollow structures (at 200°C) and foaming (at 175°C) that were observed in our work can be explained as follows. At 200°C, the L_1L_2 region is smaller and is shifted more toward the solvent side of the phase diagram in comparison with higher temperatures (see Figs. 5 and 6), so vapor-phase nucleation at the L_1L_2V line occurs only shortly after the formation

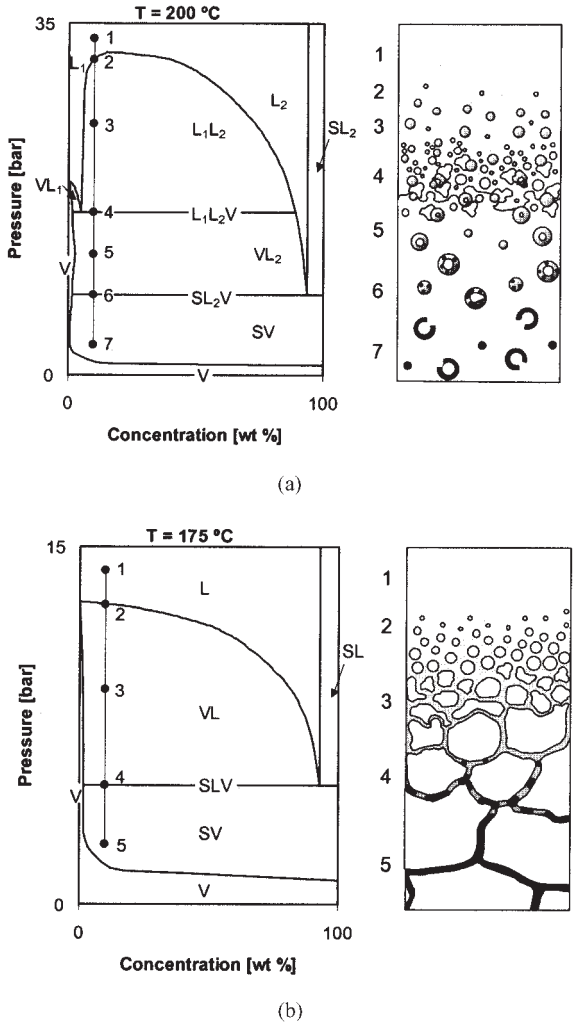

Figure 11 Pressure–composition diagrams and expected phase transitions during rapid expansion for CTA–EA solutions at (a) 200 and (b) 175°C. An isothermal rapid-expansion path at a constant composition is depicted on the phase diagram; the resulting phase transitions that occur along the expansion path are shown to the right.

of the polymer-rich phase L_2, which is still relatively rich in solvent. Any vapor phase that nucleates inside the L_2 phase will expand it into the hollow structures that were experimentally observed and are shown in the illustration at 7 in Figure 11(a). At 175°C, the situation is somewhat different. As shown in Figures 5 and 11(b), there is no liquid–liquid region, so the vapor nuclei form directly within the solvent-rich, homogeneous solution being expanded. The expansion of the vapor bubbles trapped within this low-viscosity liquid phase causes the foaming observed at 175°C (and not at any other temperature).

For the rapid expansion of saturated, two-phase mixtures, our solutions will phase-separate in the pre-expansion section before entering the nozzle. (Zhuang and Kiran[26] showed that polymer–solvent phase separation could occur in milliseconds under appropriate conditions, and the residence times in our pre-expansion section are 2–4 s.) Thus, the polymer-rich droplets (L_2) will have ample opportunity to coalesce into larger structures before a significant pressure drop has occurred and the vapor phase nucleates inside the nozzle. No hollow structures are formed because vapor nucleation occurs within the solvent-rich liquid phase L_1, external to the volumes of the polymer-rich liquid phase (L_2). The polymer-rich liquid volumes formed upstream of the nozzle then solidify into the relatively large structures observed in our work. Finally, the fact that all two-phase mixtures were expanded at temperatures well above the LCEP also may explain why no hollow structures or foaming was observed.

Our explanation of why concentration is the controlling variable for product morphology has been given elsewhere,[14] so it is only summarized here. For two-phase solutions, polymer-rich volumes are relatively small at low polymer concentrations (e.g., 0.5 wt %), and when sheared within the nozzle, they remain in droplet form. For higher concentrations (e.g., 5 wt %), the polymer-rich volumes are large enough to be drawn into fibers by the shear flow. For the expansion of unsaturated solutions, a higher polymer concentration increases the likelihood that condensation and coagulation can take place as the rapid-expansion process occurs within the nozzle. Shear forces are then responsible for oriented, rather than isotropic, growth.

CONCLUSIONS

When used as a hot, compressed liquid at approximately 175°C, EA is an effective solvent for CTA and can, therefore, be used as a replacement for methylene chloride in CTA fiber and film processing. No undesirable side reactions were detected at the elevated temperatures of operation. Furthermore, CTA remains dissolved in EA after the solution is cooled to ambient conditions, which suggests that CTA fibers can be manufactured from CTA–EA solutions with conventional dry-spinning equipment.

Although ethanol dissolved CTA at approximately 165°C, the nucleophilic substitution reaction with CTA produced significant amounts of EA as a byproduct. Additional work would be required to determine whether a reduction in residence times at elevated temperatures from hours to minutes would eliminate this problem.

On the basis of this work and our earlier study using a CO_2–fluoropolymer system, the relationship between the RESS processing conditions and product morphologies can now be seen to be influenced by two factors: the polymer concentration and the polymer–solvent phase behavior. Thus, although a minimum polymer concentration (i.e., ~5 wt %) is necessary for the production of fibers, we have discovered an additional constraint: the rapid-expansion path must include penetration into a region of LLE. Furthermore, this region must be large enough for the polymer-rich phase to have time to adequately develop before the onset of VLE at lower pressures. (Expansion can begin either in the two-phase LLE region or at pressures above the LLE region, at which the initial solution is homogeneous.) For example, the rapid expansion of a 5 wt % CTA–EA solution at 250°C and 69 bar, that is, at a temperature and a pressure well above the LCEP and three-phase LLV line, respectively, produced large amounts of continuous CTA fibers. On the other hand, RESS of a 5 wt % solution at 200°C and 69 bar, at which the LLE region encompassed a pressure range of only about 10 bar before the onset of VLE, showed few fibers and many hollow structures produced by vapor expansion in the polymer-rich phase. At temperatures below the LCEP, at which there was no region of LLE, foams were produced, as vapor bubbles formed directly from the initially homogeneous solution of CTA and EA.

At lower polymer concentrations (e.g., 2 wt %), at which particles were the dominant product morphology, the system phase behavior similarly impacted the product morphology, as solid particles were formed at 250°C and 69 bar, and particles disrupted by vapor expansion were formed at 200°C and 69 bar.

The authors are grateful to the following people at Clemson for their assistance: Jaouad Meziani for X-ray powder diffraction, differential scanning calorimetry, and thermogravimetric analysis; Chris O'Brien for gas chromatography/mass spectrometry analysis; and Kimberley Ivey for Fourier transform infrared measurements. The authors also thank Markus Weber of Degussa AG (Germany), who designed the type-II nozzle in this work.

References

1. Petersen, R. C.; Matson, D. W.; Smith, R. D. J Am Chem Soc 1986, 108, 2100.

2. Lele, A. K.; Shine, A. D. AIChE J 1992, 38, 742.
3. Williams, J. R.; Clifford, A. A.; Bartle, K. D.; Kee, T. P. Powder Technol 1998, 96, 158.
4. Türk, M.; Hils, P.; Helfgen, B.; Schaber, K.; Martin, H.-J.; Wahl, M. A. J Supercrit Fluids 2002, 19, 327.
5. Tom, J. W.; Debenedetti, P. G.; Jerome, R. J Supercrit Fluids 1994, 7, 9.
6. Charoenchaitrakool, M.; Dehghani, F.; Foster, N. R.; Chan, H. K. Ind Eng Chem Res 2000, 39, 4794.
7. Alessi, P.; Cortesi, A.; Kikic, I.; Foster, N. R.; Macnaughton, S. J.; Colombo, I. Ind Eng Chem Res 1996, 35, 4718.
8. Shim, J.-J.; Yates, M. Z.; Johnston, K. P. Ind Eng Chem Res 1999, 38, 3655.
9. Chernyak, Y.; Henon, F.; Harris, R. B.; Gould, R. D.; Franklin, R. K.; Edwards, J. R.; DeSimone, J. M.; Carbonell, R. G. Ind Eng Chem Res 2001, 40, 6118.
10. Petersen, R. C.; Matson, D. W.; Smith, R. D. Polym Eng Sci 1987, 27, 1693.
11. Lele, A. K.; Shine, A. D. Ind Eng Chem Res 1994, 33, 1476.
12. Mawson, S.; Johnston, K. P.; Combes, J. R.; DeSimone, J. M. Macromolecules 1995, 28, 3182.
13. Aniedobe, N. E.; Thies, M. C. Macromolecules 1997, 30, 2792.
14. Blasig, A.; Shi, C.; Enick, R. M.; Thies, M. C. Ind Eng Chem Res 2002, 41, 4976.
15. Gedon, S.; Fengl, R. Kirk-Othmer Encyclopedia of Chemical Technology, 4th ed.; Wiley: New York, 1993; Vol. 5, p 496.
16. Moch, I., Jr. Kirk-Othmer Encyclopedia of Chemical Technology, 4th ed.; Wiley: New York, 1993; Vol. 13, p 312.
17. Serad, G. A. Kirk-Othmer Encyclopedia of Chemical Technology, 4th ed.; Wiley: New York, 1993; Vol. 10, p 598.
18. Mackenzie, K. J. Kirk-Othmer Encyclopedia of Chemical Technology, 4th ed.; Wiley: New York, 1993; Vol. 10, p 761.
19. Lee, S.-H.; LoStracco, M. A.; McHugh, M. A. Macromolecules 1996, 29, 1349.
20. Ambrose, D.; Ellender, J. H.; Gundry, H. A.; Lee, D. A.; Townsend, R. J. Chem Thermodyn 1981, 13, 795.
21. Elliott, J. R.; Lira, C. T. Introductory Chemical Engineering Thermodynamics; Prentice-Hall: Upper Saddle River, NJ, 1999; p 445.
22. Hong, L.; Thies, M. C.; Enick, R. M. J Supercrit Fluids, submitted.
23. Scott, R. L.; van Konynenburg, P. H. Discuss Faraday Soc 1970, 49, 87.
24. Blasig, A. Ph.D. Dissertation, Clemson University, 2004.
25. Weber, M.; Thies, M. C. In Supercritical Fluid Technology in Materials Science and Engineering: Synthesis, Properties, and Applications; Sun, Y.-P., Ed.; Marcel Dekker: New York, 2002; p 387.
26. Zhuang, W.; Kiran, E. Polymer 1998, 39, 2903.